Received: 17 November 2019 | Accepted: 26 May 2020
DOI: 10.1002/asna.202013701

Astronomische Nachrichten

ORIGINAL ARTICLE

The nature of active galaxies based on their radio properties

Hayk V. Abrahamyan

NAS RA V. Ambartsumian Byurakan, Astrophysical Observatory (BAO), Byurakan, Armenia

Correspondence
Hayk V. Abrahamyan, NAS RA V. Ambartsumian Byurakan, Astrophysical Observatory (BAO), Byurakan, 0213, Aragatzotn Province, Armenia.
Email: abrahamyanhayk@gmail.com

Abstract

In this paper, we investigate radio properties of active galaxies taken from the reference [Véron-Cetty & Véron (2010)] catalog. The galaxies are limited to magnitudes in the range of $12^m - 19^m$. We have cross-correlated the list with radio catalogs and selected those galaxies that have data on six or more radio fluxes at different wavelengths. As a result, we have 198 galaxies that satisfy these conditions. Using SDSS DR15, we have obtained 96 spectroscopic identifications of the 198 objects. After the classification, 85% of the 96 objects have changed their types. Available data on the classification of these objects and our classification showed that 56.7% of them are Seyfert galaxies. For all the objects, we have built radio spectra and estimated radio spectral indices. As a result, we obtain $\overline{\alpha} = -0.6089 \pm 0.056(\overline{\alpha}_{\mathrm{Seyfert}} = -0.6013 \pm 0.027$, $\overline{\alpha}_{\mathrm{LINER}} = -0.5955 \pm 0.025$, $\overline{\alpha}_{\mathrm{HII}} = -0.6672 \pm 0.039$, $\overline{\alpha}_{\mathrm{Comp.}} = -0.7128 \pm 0.043)$. We discuss the radio properties of active galaxies based on their radio spectral indices.

KEYWORDS

AGN, LINER, QSO, radio galaxy, radio spectral index, Seyfert

1 | INTRODUCTION

In terms of activity, most of the galaxies in the Universe are considered "normal", without any prominent activity manifestation. Normal galaxies have total luminosities up to about $10^{11} \times L_{\mathrm{Sun}}$. For example, all galaxies in the Local Group (including the Milky Way and Andromeda Galaxy) are normal ones. In the spectra of normal galaxies, we observe the sum of spectra of all the stars the galaxy contains. The luminosity of normal galaxies does not change much in short periods of time.

Active galaxies are among the most interesting objects in the Universe. They have higher luminosities than normal galaxies. It is important that active galaxies have brighter nuclei than normal ones. In these galaxies, large amounts of energy are obtained from such small areas as the galactic nuclei. A massive or supermassive black hole is considered to be present in the center of each of these galaxies. Some active galaxies have gigantic jets in optical and, more often, in radio ranges. The luminosity of an active galaxy can change twice and even more times during a short period of time, for instance, some active galaxies show variability during a period of a few days.

Active galaxies are of different types: radio galaxies, Seyfert galaxies, quasars, blazars, low-ionization narrow emission-line regions (LINERs), and others. Radio galaxies are elliptical galaxies. All galaxies radiate some radio waves. In case of normal galaxies, radio emission corresponds to a small fraction of the total energy radiated by the galaxy. The energy for radio galaxies radiated at radio wavelengths is 0.1–10 times more than the energy radiated at visible wavelengths. Seyfert galaxies were discovered by Carl Seyfert (1943). These galaxies have broad emission-line spectra indicating cores of hot, low-density ionized gas. The "typical" members of the class (Seyfert 1 and 2) were described by Khachikian & Weedman (1971, 1974).

This work is dedicated to radio properties of active galaxies. In the radio range, radio spectra of these objects are very interesting. The radio emission of a distant galaxy consists of thermal and synchrotron contributions. The thermal emission is radiation from HII regions, while the nonthermal synchrotron emission is generated by Supernova remnants (Biermann 1976; Blandford & Königl 1979; Condon 1992; De Young 1976), as well as by the core. These emission components are characterized by different spectral indices, and therefore, the total spectral index depends on their relative contributions. The radio spectral index is a powerful probe for classifying cosmic radio objects and understanding the origin of the radio emission.

To understand physical properties of some active galaxies, we have built radio spectra for our objects (spectral energy distribution) and estimate radio spectral indices (Hawkins 2002; Ulrich 1999). A radio spectral index is the most important property of radio sources in the radio range.

There are many papers devoted to radio investigation of active galaxies. Below, we present some of the recent works, which we have used and made comparisons with.

Tiwari (2019) computed the radio spectral index from a catalog of about half a million common sources in 1.4 GHz NRAO VLA Sky Survey (NVSS) and TIFR giant metrewave radio telescope (GMRT) Sky Survey.

Michal Zajaček et al. (2019) were able to infer the two-point radio spectral index distributions for star-forming galaxies, composite galaxies (with a combined contribution to the line emission from the star-formation and AGN activity), Seyferts, and LINER galaxies.

Gasperin et al. (2017) made the radio spectral index catalog and radio spectral index map public.

Rocco Coppejans et al. (2017) presented new multifrequency GMRT observations $\nu < 1$ GHz of eight $z > 4.5$ very long baseline interferometry sources.

Laing and Bridle (2013, 2014) presented accurate, spatially resolved imaging of radio spectra at the bases of jets in 11 low-luminosity (Fanaroff–Riley I) radio galaxies, derived from very large array (VLA) observations, and estimated radio spectral indices.

Abrahamyan et al. (2014) investigated the radio sources in the 7C II field and estimated radio spectral indices for 26 radio sources.

In this work, we have investigated 198 active galaxies, which also have activity in the radio range.

TABLE 1 Active galaxies in VCV-13 by activity types, excluding quasars

Activity type	Number
Seyfert	23,258
Low-ionization narrow emission-line region	907
HII	167
Unk.	9,899
Total	34,231

2 | INVESTIGATED DATA

We use data from the Véron-Cetty & Véron (2010) catalog (VCV-13). This catalog includes 133,336 quasars, 1,374 BL Lac objects, and 34,231 active galaxies (including 16,517 Seyfert 1.0). We have considered 34,231 active galaxies for our research. More information on these objects is given in Table 1.

The VCV-13 catalog was published by Véron-Cetty & Véron in 2010. It is a unique catalog that includes objects having active galaxy types. Active galaxies collected until 2010 are given. After that, no similar catalog that included active galaxies was published. Souchay et al. (2019) created the LQAC-5 catalog, which included all quasars discovered by all surveys, but it comprised only those active galaxies that were given in VCV-13. So far, we have the list of active galaxies from VCV-13.

For investigation, galaxies with magnitudes in the range of $12^m - 19^m$ have been taken. In the next step, we have cross-correlated (Abrahamyan et al. 2015) these objects with radio catalogs: FIRST (Helfand et al. 2015), NVSS (Condon et al. 1998), 87GB (Gregory & Condon 1991), GB6 (Gregory et al. 1996), 3C (Edge et al. 1959), 4C (Pilkington & Scott 1965), 7C (Hales et al. 2007), 8C (Hales et al. 1995), 9C (Waldram et al. 2003), 10C (Consortium et al. 2011), SUMSS (Mauch et al. 2003), WISH (De Breuck et al. 2002), WENSS (de Bruyn et al. 1998), Molonglo Reference Catalogue of Radio Sources (Large et al. 1991), Texas Survey of radio sources at 365 MHz (Douglas et al. 1996), Miyun 232 MHz survey (Zhang et al. 1997), CLASS survey of radio sources (Myers et al. 2003), 74 MHz VLA Low-frequency Sky Survey Redux (Lane et al. 2014), and the GMRT 150 MHz all-sky radio survey (Intema et al. 2017).

As a result, we have 4,437 objects that have been radio-identified (Table 2).

As seen from Table 2, 4,437 objects have 1–10 radio fluxes at different wavelengths. In this work, radio catalogs that cover the 38 MHz to 15.7 GHz frequency range have been used. For our investigation, we have taken objects that have six or more radio fluxes at different wavelengths.

TABLE 2 Number of identifications for active galaxies

Identification number with radio catalog	Number of objects
10	6
9	10
8	33
7	58
6	91
5	116
4	139
3	361
2	629
1	2,994
Total	4,437

TABLE 3 Activity types of active galaxies (using VCV-13, BZCAT v.5, SDSS DR15, and NED catalogs)

Activity type	Number	Percentage
Seyfert	157	79.3
Low-ionization narrow emission-line region	25	12.6
HII	4	2.0
AGN	8	4.0
Unk.	4	2.0
Total	198	100.0

With six and more radio fluxes, there is an opportunity to better understand some physical properties in radio. So, we have 198 objects with six or more radio fluxes.

3 | OPTICAL CLASSIFICATION

In order to understand some physical properties of active galaxies, we must see what activity type they have. Using the catalog VCV-13 (Véron-Cetty & Véron 2010), SDSS DR15 (Aguado et al. 2019), BZCAT v.5 (Massaro et al. 2015), and NED, we identify the activity types our objects have. In Table 3, we can see that 79% of these objects are Seyfert galaxies.

In Table 3, we have given only the information on the classification that our sources used until this work. Using the SDSS DR15 (Aguado et al. 2019) catalog, we have 96 spectroscopic identifications from our 198 sources and have carried out new classification (Abrahamyan et al. 2020, submitted).

TABLE 4 Activity type of active galaxies with our new classification

Activity type	Number	Percentage
Seyfert	112	56.7
Low-ionization narrow emission-line region	47	23.7
HII	8	4.0
Composite	21	10.6
AGN	4	2.0
Em	5	2.5
Abs	1	0.5
Total	198	100.0

We have used several methods to classify our spectra (Mickaelian et al. 2018):

- With the eye (taking into account all features and effects).
- By diagnostic diagram using [OIII]/H_β and [OI]/H_α ratios (Reines et al. 2013),
- By diagnostic diagram using [OIII]/H_β and [NII]/H_α ratios (Reines et al. 2013),
- By diagnostic diagram using [OIII]/H_β and [SII]/H_α ratios (Reines et al. 2013),
- Using the first, second, and third diagnostic diagrams simultaneously.

Classification with the eye has been carried out in comparison with the classification by diagnostic diagrams because not all the objects appeared on them. Roughly, we have distinguished Seyferts from LINERs by the criteria: [OIII]/$H_\beta > 4$ and AGN from HII by the criteria [SII]/$H_\alpha > 2/3$, [OI]/$H_\alpha > 0.1$ (Mickaelian et al. 2018; Reines et al. 2013).

So, 85% of 96 objects changed classification (Abrahamyan et al. 2020, submitted). Table 4 presents our new classification.

As a result, using Table 4, we can see that 56.7% of these objects are Seyfert galaxies, and 10.6% are Composite and have spectra close to Seyfert galaxies. Before our classification, four objects did not belong to any type (Table 3). Having spectra from SDSS, we have carried out classification for all the objects (Table 4).

In Figure 1, we have built redshift distribution for all active galaxies, Seyfert, LINER, HII, and Composite. Distribution of redshift for AGN, Em, and Abs has not been demonstrated as we have small numbers of these types of galaxies (Table 4). The top curve (black line) shows

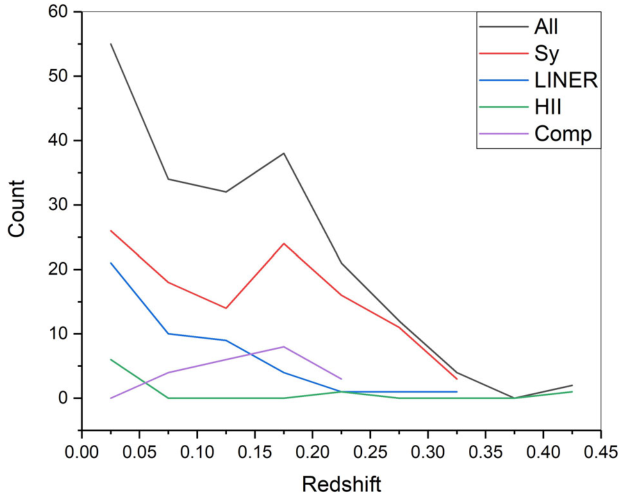

FIGURE 1 Distribution of redshifts

the sum of all types of galaxies in the figure (included Seyfert, LINER, HII, Composite, AGN, Em, and Abs). Above $z \sim 0.33$, there are not only HII but also AGN, Em, and Abs.

Using Figure 1, we can see that our objects have redshifts in the range of 0.001–0.418. In this distribution, the number of objects increases from 0.075 to 0.0175 redshifts. However, the number of objects that condition this increase is very small (five objects) and, hence, has been neglected.

4 | ABSOLUTE MAGNITUDE AND LUMINOSITY

Aiming at understanding some optical properties and the way they can be connected with radio properties, we have computed absolute magnitudes and luminosities for our objects (Abrahamyan et al. 2019). For our absolute magnitude computation, we have used V-band from VCV-13 (Véron-Cetty & Véron 2010) and taken redshift from SDSS DR15 (Aguado et al. 2019) if there is spectroscopic identification.

We have counted absolute magnitudes for our active galaxy using Formula (1) (Véron-Cetty & Véron 2010).

$$M = m + 5 - 5 \times \mathrm{Log}D - f(z) + \Delta m(z) \quad (1)$$

where D (Formula 2) is the luminosity distance as defined by Riess et al. (2004):

$$D = \frac{c \times (1+z)}{H_0} \times \int_0^z [(1+z)^3 \times \Omega_M + \Omega_\Lambda]^{-0.5} dz \quad (2)$$

z is the redshift, $f(z) = -2.5 \times \log(1+z)^{1-\alpha}$ the $f(z)$ correction, and $\Delta m(z)$ is a correction to $f(z)$ considering that the spectrum of quasars is not strictly a power law of the form $S \sim \vartheta^{-\alpha}$ ($\alpha = 0.3$, Véron-Cetty & Véron 2010).

The following values have been taken for the cosmological constants in the calculations (Aghanim et al. 2018; Zhang & Qing-Guo 2018): $\Omega_M = 0.29$, $\Omega_\Lambda = 0.71$, $H_0 = 71$ km $\times$ s^{-1}/Mpc.

Having absolute magnitude, we have counted the luminosities using Formula (3) (Abrahamyan et al. 2019).

$$L = L_\odot \times 2.512^{M_\odot - M} \quad (3)$$

where $L_\odot$ and $M_\odot$ are luminosity and absolute magnitude of Sun, respectively ($L_\odot = 3.83 \times 10^{33}$ erg/s, $M_\odot = 4.83$).

In Table 5, we give average luminosity and absolute magnitude for our active galaxies.

Having absolute magnitude, we have built the dependence of absolute magnitude on redshift graph (Figure 2).

In Figure 2, we can see that, on average, LINERs are closer than Seyferts, and Seyfert galaxies are brighter than LINERs on average (Table 5). LINER is a type of galactic nucleus that is defined by its spectral line emission (Heckman 1980). The spectra typically include line emission from low ionization or neutral atoms.

Having information on magnitude from SDSS DR15 (Aguado et al. 2019), we have built color–magnitude and color–color diagrams for our objects (Figures 3 and 4).

TABLE 5 Absolute magnitude and luminosity

Types	Luminosity range (erg/s)	Average luminosity (erg/s)	Absolute magnitude range	Average absolute magnitude
Seyfert	$5.01 \times 10^{42} \div 8.38 \times 10^{44}$	8.08×10^{43}	$-17.98 \div -23.52$	-20.98
Low-ionization narrow emission-line region	$1.78 \times 10^{42} \div 3.46 \times 10^{44}$	4.20×10^{43}	$-16.84 \div -22.56$	-20.27
HII	$7.23 \times 10^{42} \div 1.87 \times 10^{44}$	3.91×10^{43}	$-18.36 \div -21.89$	-20.13
Composite	$2.17 \times 10^{43} \div 1.21 \times 10^{44}$	4.48×10^{43}	$-19.55 \div -21.42$	-20.34
All	$1.78 \times 10^{42} \div 8.38 \times 10^{44}$	5.75×10^{43}	$-16.84 \div -23.52$	-20.61

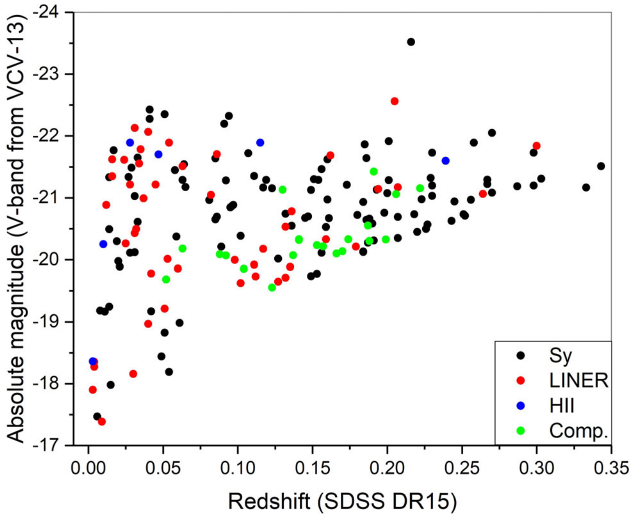

FIGURE 2 Absolute magnitude (V-band from VCV-13) versus redshift (SDSS DR15)

Studying the diagrams one can get some insight into our objects (Figures 3 and 4). On average, Seyfert galaxies are blue, while LINERs are red. Other classes (HII, Comp.) are almost evenly distributed on diagrams.

Thus, the separation of our objects by this method gives an opportunity to realize that objects having powerful radio sources are mainly of two types: Seyfert galaxies and LINERs. Using that, the comparison has been mainly drawn between these two types.

5 | RADIO PROPERTIES OF ACTIVE GALAXIES

5.1 | Radio spectral index

Active galaxies are very interesting objects in the Universe. In order to understand some physical properties, we must identify which properties our objects have in radio range. We have 198 active galaxies with six or more radio fluxes at different wavelengths. A very important radio property for radio objects is the radio spectral index. It shows steep radio spectra. Using six or more frequencies, we have developed a graph for all 198 galaxies (lg[flux] vs. lg[frequencies]). Using an lg[flux] versus lg[frequencies] graph for each source, we have made linear fitting. The software "Origin" gives the formula for each linear fit, and using that, we have measured the radio spectral index for each source. The plot shows steep radio spectra for each line, and that is considered radio spectral index. As examples, we give average radio spectra for our objects in Figure 5.

In Figure 5, average radio spectra for different types of our objects are given. These average spectra are normalized by the Texas Survey, and the scale is fitted to average the radio spectra of Seyfert galaxies. It is obvious that HII and Composite, on average, have steeper radio spectra than Seyferts and LINERs (Table 7).

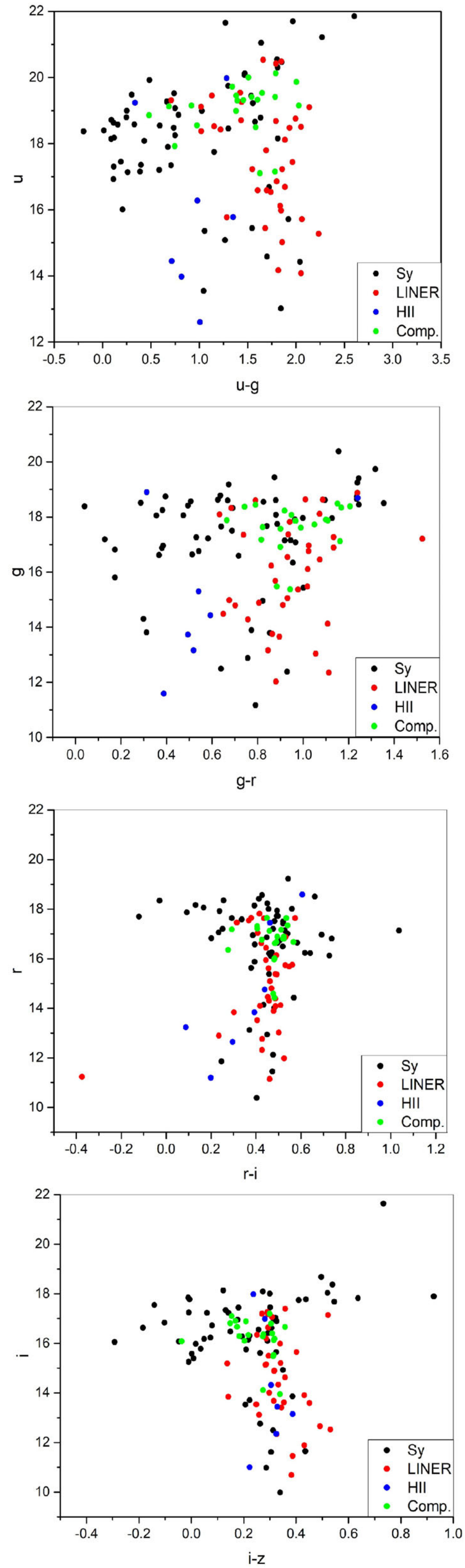

FIGURE 3 Color–magnitude diagrams

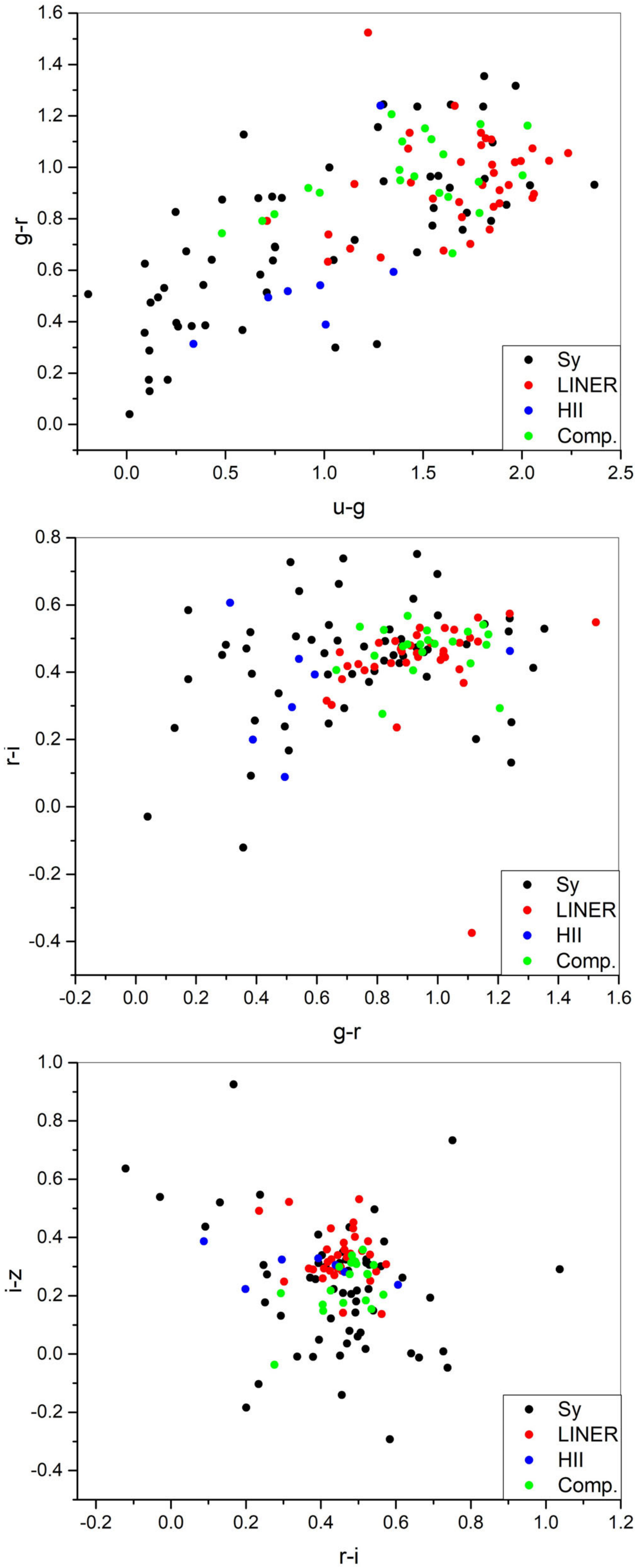

FIGURE 4 Color–color diagrams

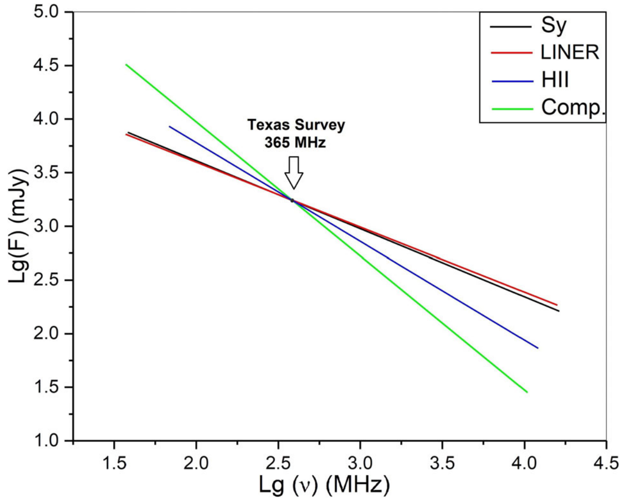

FIGURE 5 Average radio spectra for our object

Several authors have estimated the radio spectral index for quasars and radio galaxies. In our work, we have estimated radio spectral indices for 198 radio objects and compared our results with some authors (e.g., with Abrahamyan et al. 2014, Tiwari 2019, etc.).

Using 198 spectra of our radio objects, we have estimated radio spectral indices. For radio spectral index errors, in the first step, we have counted each point's (radio flux) shift from fitting line in spectra. Using the shift of each point, we have estimated errors in the radio spectral index using Formula (4).

$$\sigma_{\text{error}} = \sqrt{\frac{\sum_{i=1}^{n} k_n^2}{n}} \tag{4}$$

where σ_{error} is the error of radio spectral index, k_n is the shift of each point from fit (Figure 5), and n is the number of measurements.

Table 6 presents information on radio spectral indices, absolute magnitude, and luminosity.

So, radio spectral indices for 198 objects have been estimated using spectra. For this, we have built distribution of spectral indices (Figure 6).

In Figure 6, we can see two peaks at −0.75 and −0.35, but the growth is observed in five sources, and we neglect it; hence, we can note that our active galaxies mainly have steep radio spectra ($-0.9 < \alpha < -0.5$).

Table 7 illustrates the average information of radio spectral indices.

Using information from Table 7, we can see that Seyfert galaxies and LINERs have the same radio spectra on average, but HII has steeper radio spectra than Seyferts and LINERs. In fact, we have investigated the low-frequency radio range, mostly lower than 1,420 MHz. That is why HII regions show steeper radio indices compared to Seyferts and LINERs.

TABLE 6 Information of radio spectral indices, absolute magnitude, and luminosity (for 30 objects, all tables are given in VIZIER)

N	RAJ2000 deg	DEJ2000 deg	Redshift	Activity type old	Activity type new	Absolute magnitude	L (erg/s) $\times 10^{43}$	Radio sp. index	Radio sp. index (error)
1	005.305000	−19.178889	0.095	Sy1.9	Sy1.9	−20.84	7.127	−0.6561	0.052
2	006.673750	35.145278	0.333	Sy2	Sy2	−21.16	9.578	−0.37027	0.033
3	007.139167	00.919444	0.104	Sy2	S2.0/LINER	−19.85	2.865	−0.87907	0.035
4	007.841667	30.266944	0.2	Sy1	Sy1	−21.08	8.835	−0.52622	0.047
5	010.200833	−20.727500	0.092	Sy	Sy	−21.28	10.647	−0.34856	0.045
6	010.210833	10.057778	0.188	Sy1	Sy1	−20.66	6.034	−0.68925	0.034
7	011.145417	12.186389	0.226	Sy1	Sy1	−20.50	5.185	−0.76769	0.046
8	011.888333	−25.288056	0.001	Sy	Sy	−18.00	0.502	−0.14928	0.033
9	012.196667	31.956944	0.014	Sy1h/BZG	Sy1h/BZG	−19.24	1.633	−0.23939	0.031
10	014.004167	68.375278	0.184	Sy2	Sy2	−20.93	7.739	−0.68569	0.041
11	014.454583	30.353056	0.016	LINER	LINER	−21.62	14.576	−0.32732	0.043
12	015.523750	14.723611	0.188	Sy2	S2.0/LINER	−20.30	4.331	−0.72183	0.058
13	025.491250	39.391667	0.08	Sy1/BZU	Sy1/BZU	−21.64	14.797	−0.33153	0.031
14	025.579167	13.462778	0.267	Sy1	S1.5	−21.22	10.099	−0.83292	0.050
15	027.067917	00.329167	0.092	Sy1	S1.9/LINER	−20.07	3.493	−0.59974	0.036
16	031.759583	29.512778	0.111	Sy1.8	Sy1.8	−21.35	11.395	−0.65316	0.046
17	035.226250	−01.947500	0.173	Sy2	Sy2	−21.21	9.971	−0.85782	0.043
18	035.798333	42.992500	0.021	Sy1	Sy1	−19.89	2.965	−0.82192	0.074
19	035.802917	86.320556	0.184	Sy2	Sy2	−20.12	3.670	−0.95187	0.076
20	036.261667	−23.213333	0.23	Sy1	Sy1	−21.03	8.459	−0.85423	0.060
21	036.364167	37.174444	0.033	Sy/BZG	Sy/BZG	−21.65	14.989	−0.31915	0.054
22	041.579167	−30.274444	0.004	LINER	LINER	−18.35	0.719	−0.46073	0.051
23	042.899583	43.253333	0.051	LINER	LINER	−19.21	1.587	0.2206	0.029
24	045.426667	35.205833	0.016	LINER	LINER	−21.35	11.367	−0.45459	0.032
25	045.716250	−18.406667	0.089	Sy2	Sy2	−20.21	3.986	−0.61696	0.037
26	047.109167	04.110833	0.029	Sy1	Sy1	−21.49	12.897	−0.43542	0.057
27	047.500833	17.099444	0.256	Sy2	Sy2	−20.97	7.998	−0.83648	0.092
28	048.110833	39.275000	0.161	Sy1.0	Sy1.0	−20.67	6.089	−0.68189	0.075
29	048.258750	41.333611	0.136	Sy1/BZU	Sy1/BZU	−20.55	5.438	−0.11655	0.023
30	049.950833	41.511667	0.017	Sy1.5/BZU	Sy1.5/BZU	−21.77	16.732	−0.09794	0.020

Abbreviation: LINER, low-ionization narrow emission-line region.

Figure 7 shows graphical dependence of radio spectral index on redshift. In this figure, distant objects have steeper radio spectra than the near ones.

5.2 | Radio spectral index dependence on physical size

Tiwari (2019) presented the dependence of radio spectral index on angular size in his work. The size is defined as $\sqrt{ab}$ (in arcsec), where a and b are the major and minor axes of the Gaussian fit, respectively.

Using redshift information, we have estimated physical sizes for our objects. Using the formula $\tan(\theta/2) = x/2D$, where θ is the angular size of the object on the sky, "x" is the physical size of object, and "D" is the distance to the object (Formula 2), we have calculated "x" physical size for each object. For θ, the major axes of objects have been taken from catalog automated plate measurement

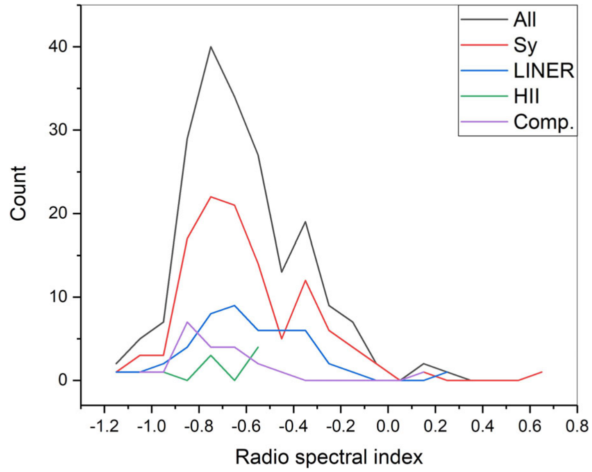

FIGURE 6 Distribution of radio spectral indices

TABLE 7 Average radio spectral indices for different types of active galaxies

Activity type	Average radio spectral index
Seyfert	−0.6013 ± 0.027
Low-ionization narrow emission-line region	−0.5955 ± 0.025
HII	−0.6672 ± 0.039
Composite	−0.7128 ± 0.043
All	−0.6089 ± 0.056

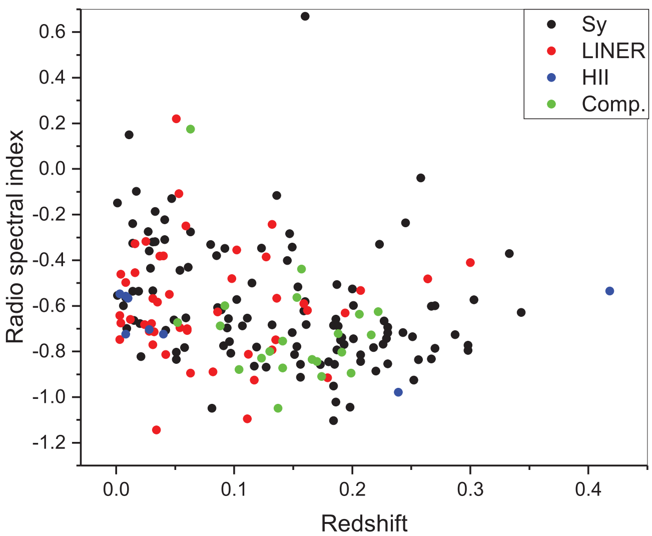

FIGURE 7 Radio spectral index versus redshift

(McMahon et al. 2000). In Table 8, information on physical sizes is given.

We have eight objects that have HII activity. For these sources, we have also estimated physical sizes, and for one of them, we have obtained very big physical size (832.2 kpc) compared to the other HII objects, which are up to 116.35 kpc. With the purpose of calculating the average size and drawing other comparisons, we have excluded this object.

TABLE 8 Physical sizes of active galaxies

Activity type	Range of sizes (kpc)	Average size (kpc)	RMS (kpc)
Seyfert	2.39 ÷ 305.46	44.88	35.62
Low-ionization narrow emission-line region	7.36 ÷ 190.19	50.15	36.14
HII	5.4 ÷ 116.35	46.81	33.81
Comp.	22.27 ÷ 107.51	50.23	22.46
All	2.39 ÷ 305.46	46.97	32.26

Therefore, using physical sizes, we have developed the dependence of radio spectral index on physical size (Figure 8).

Using Table 8 and Figure 8, we state that objects of various activity types statistically have the same average sizes.

However, due to the small number of objects, this result is statistically not substantiated; hence, we need further studies using a greater numbers of objects to follow the real differences in distributions of physical sizes for different types of active galaxies.

6 | RESULTS

Currently, we wish to understand what radio properties active galaxies have. For that reason, we have created a list of radio objects that have $12^m - 19^m$ magnitudes, and each object has six or more radio fluxes at different wavelengths. With this method, we have distinguished 198 active galaxies. Using that, we have estimated radio spectral indices for all the objects.

Similar work was carried out by Abrahamyan et al. (2014). The authors investigated 7C (Hales et al. 2007) catalogs and separated 26 radio galaxies, as well as estimated radio spectral indices of those objects. We have compared our list to the list proposed by Abrahamyan et al. (2014). As a result, the objects have not been identified. In the mentioned work, the average radio spectral index for radio galaxies had $\alpha = -0.806$, which is a little different from our present results. In this work, radio objects have been selected by another method; errors are not estimated, and they have redshifts up to $z = 3$.

Laing & Bridle (Laing & Bridle 2013) presented accurate, spatially resolved imaging of radio spectra at the bases of jets in 11 low-luminosity (Fanaroff–Riley I) radio galaxies, derived from VLA observations. The Authors showed images and profiles of the spectral index over the

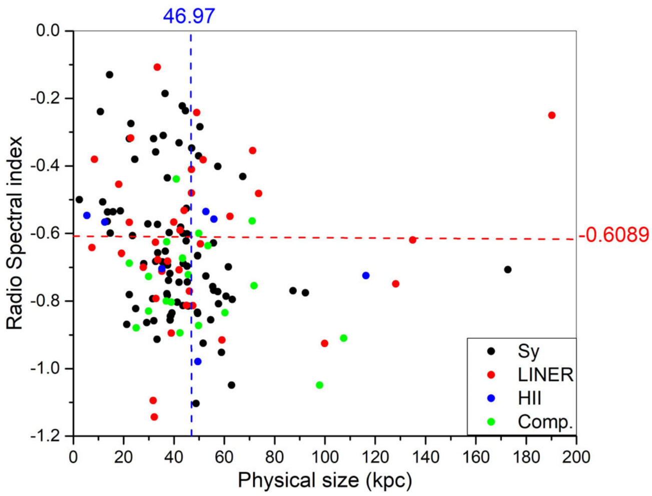

FIGURE 8 Radio spectral index versus physical size

frequency range 1.4–8.5 GHz, together with values integrated over fiducial regions defined by relativistic models of the jets. The mean spectral indices given by the authors is 0.66 ± 0.01. We have compared our result to those of Laing & Bridle (Laing & Bridle 2013), and they appear to be similar.

So far, we have given some new results for properties of active galaxies:

- Of our 198 active galaxies, 56.7% are Seyfert galaxies.
- Using SDSS DR15, we have 96 objects that have spectra. We have classified these sources, and as a result, 85% of these objects changed their classes.
- We have estimated average absolute magnitudes and luminosities (Table 5) for 198 active galaxies ($\overline{M}_{\rm Seyfert} = -20.98$, $\overline{M}_{\rm LINER} = -20.27$, $\overline{M}_{\rm HII} = -20.13$, $\overline{M}_{\rm Comp.} = -20.34$, $\overline{L}_{\rm Seyfert} = -8.08 \times 10^{43}$ erg/s, $\overline{L}_{\rm LINER} = 4.20 \times 10^{43}$ erg/s, $\overline{L}_{\rm HII} = 3.91 \times 10^{43}$ erg/s, $\overline{L}_{\rm Comp.} = 4.48 \times 10^{43}$ erg/s).
- In color–magnitude and in color–color diagrams (Figure 4), LINERs stand out from Seyfert galaxies.
- We have built radio spectra and estimated radio spectral indices for 198 active galaxies ($\overline{\alpha} = -0.6089 \pm 0.056$, $\overline{\alpha}_{\rm Seyfert} = -0.6013 \pm 0.027$, $\overline{\alpha}_{\rm LINER} = -0.5955 \pm 0.025$, $\overline{\alpha}_{\rm HII} = -0.6672 \pm 0.039$, $\overline{\alpha}_{\rm Comp.} = -0.7128 \pm 0.043$). Using information from Table 7, we can note that, on average, Seyferts and LINERs have the same radio spectra (on average), whereas HII has steeper radio spectra than Seyferts and LINERs.
- We have created dependence of radio spectral index on redshift (Figure 7). In this figure, objects that are far have steeper radio spectra than the nearby objects.
- We have estimated physical sizes (the average physical size = 46.97 ± 32.26 kpc) for our objects. Using Table 8 and Figure 8, we can state that objects of various activity types statistically have the same average sizes. However, due to small number of objects, this result is statistically not substantiated; hence, we need further studies using bigger numbers of objects to follow the real differences in distributions of physical sizes for different types of active galaxies.

REFERENCES

Abrahamyan, H. V., Andreasyan, R. R., Hovhannisyan, M. A., & Paronyan, G. M. 2014, *Astrophysics*, *57*(3), 359.
Abrahamyan, H. V., Mickaelian, A. M., & Knyazyan, A. V. 2015, *Astron. Comput.*, *10*, 99.
Abrahamyan, H. V., Mickaelian, A. M., Paronyan, G. M., & Mikayelyan, G. A. 2019, *AN*, *340*(5), 437.
Abrahamyan, H. V., Mickaelian, A. M., Paronyan, G. M., & Mikayelyan, G. A. 2020, *Astrophysics submitted*, *3*.
Aghanim, N., Akrami, Y., Ashdown, M., Aumont, J., Baccigalupi, C., & et al. 2018, eprint arXiv:1807.06209, https://arxiv.org/abs/1807.06209.
Aguado, D. S., Ahumada, R., Almeida, A., Anderson, S. F., et al. 2019, *A&AS*, *240*(2), 23.
Biermann, P. 1976, *A&A*, *53*, 295.
Blandford, R. D., & Königl, A. 1979, *ApJ*, *232*, 34.
Condon, J. J. 1992, *ARA&A*, *30*, 575.
Condon, J. J., Cotton, W. D., Greisen, E. W., Yin, Q. F., Perley, R. A., et al. 1998, *AJ*, *115*(5), 1693.
Consortium, D. M. L., Franzen, T. M. O., Waldram, E. M., Grainge, K. J. B., et al. 2011, *MNRAS*, *415*(3), 2708.
Coppejans, R., van Velzen, S., Intema, H. T., et al. 2017, *MNRAS*, *462*(2), 2039.
De Breuck, C., Tang, Y., de Bruyn, A. G., Rottgering, H., & van Breugel, W. 2002, *A&A*, *394*, 59.
de Bruyn, G., Miley, G., Rengelink, R., Tang, Y., et al. 1998, *VizieR On-line Data Catalog: VIII/62*, WENSS Collaboration NFRA/ASTRON and Leiden Observatory, Netherland.
de Gasperin, F., Intema, H. T., & Frail, D. A. 2017, *MNRAS*, *474*(4), 5008.
De Young, D. S. 1976, *ARA&A*, *14*, 447.
Douglas, J. N., Bash, F. N., Bozyan, F. A., Torrence, G. W., & Wolfe, C. 1996, *AJ*, *111*, 1945.
Edge, D. O., Shakeshaft, J. R., McAdam, W. B., Baldwin, J. E., & Archer, S. 1959, *Mem. R. Astronom. Soc.*, *68*, 37.
Gregory, P. C., & Condon, J. J. 1991, *AJS*, *75*, 1011.
Gregory, P. C., Scott, W. K., Douglas, K., & Condon, J. J. 1996, *AJS*, *103*, 427.
Hales, S. E. G., Riley, J. M., Waldram, E. M., Warner, P. J., & Baldwin, J. E. 2007, *MNRAS*, *382*(4), 1639.
Hales, S. E. G., Waldram, E. M., Rees, N., & Warner, P. J. 1995, *MNRAS*, *274*(2), 447.
Hawkins, M. R. S. 2002, *MNRAS*, *329*(1), 76.
Heckman, T. M. 1980, *A&A*, *87*, 152.
Helfand, D. J., White, R. L., & Becker, R. H. 2015, *AJ*, *501*(1), 26.
Intema, H. T., Jagannathan, P., Mooley, K. P., & Frail, D. A. 2017, *A&A*, *598*, A78.
Khachikian, E. E., & Weedman, D. W. 1971, *Astrophysics*, *7*, 231.
Khachikian, E. E., & Weedman, D. W. 1974, *ApJ*, *192*, 581.
Laing, R. A., & Bridle, A. H. 2013, *MNRAS*, *432*, 1114.
Laing, R. A., & Bridle, A. H. 2014, *MNRAS 43*, 3405.

Lane, W. M., Cotton, W. D., van Velzen, S., et al. 2014, *MNRAS*, *440*(1), 327.
Large, M. I., Cram, L. E., & Burgess, A. M. 1991, *Observatory*, *111*, 72.
Massaro, E., Maselli, A., Leto, C., Marchegiani, P., Perri, M., Giommi, P., & Piranomonte, S. 2015, *Astrophys. Space Sci.*, *357*(1), 75.
Mauch, T., Murphy, T., Buttery, H. J., et al. 2003, *MNRAS*, *342*(4), 117.
McMahon, R. G., & McMahon, M. M., M Irwin. 2000, *The APM-North Catalogue*.
Mickaelian, A. M., Harutyunyan, G. S., & Sarkissian, A. 2018, *Astron. Lett.*, *44*, 6.
Myers, S. T., Jackson, N. J., Browne, I. W. A., et al. 2003, *MNRAS*, *341*(1), 1.
Pilkington, J. D. H., & Scott, J. F. 1965, *Mem. R. Astronom. Soc.*, *69*, 183.
Reines, A. E., Greene, J. E., & M., G. 2013, *AJ*, *755*, 2.
Riess, A. G., Strolger, L.-G., Tonry, J., et al. 2004, *ApJ*, *607*, 665.
Seyfert, C. K. 1943, *AJ*, *97*, 28.
Souchay, J., Gattano, C., Andrei, A. H., et al. 2019, *A&A*, *624*, A145.
Tiwari, P. 2019, *RAA*, *19*(7), 96.
Ulrich, M.-H. 1999, *Contribution for the Encyclopedia of Astronomy and Astrophyisics*, *Oxford Institute of Physics and MacMillan*, Oxford, England.
Véron-Cetty, M. P., & Véron, P. 2010, *A&A*, *A10*, 518.
Waldram, E. M., Pooley, G. G., Grainge, K. J. B., Jones, M. E., Saunders, R. D. E., Scott, P. F., & Taylor, A. C. 2003, *MNRAS*, *342*(3), 915.
Zajaček, M., Busch, G., Valencia-S, M., et al. 2019, *A&A*, *A83*, 630.
Zhang, X., & Qing-Guo H. 2018, eprint arXiv:1812.01877, https://arxiv.org/abs/1812.01877.
Zhang, X., Zheng, Y., Chen, H., Wang, S., Cao, A., Peng, B., & Nan, R. 1997, *A&AS*, *121*, 59.

AUTHOR BIOGRAPHY

Hayk V. Abrahamyan, NAS RA V. Ambartsumian Byurakan, Astrophysical Observatory (BAO), Byurakan, 0213, Aragatzotn Province, Armenia

How to cite this article: Abrahamyan HV. The nature of active galaxies based on their radio properties. *Astron. Nachr.*. 2020;1–10. https://doi.org/10.1002/asna.202013701